

DEVELOPMENT AND IMPLEMENTATION OF A TECHNIQUE FOR FAST FIVE-HOLE PROBE MEASUREMENTS DOWNSTREAM OF A LINEAR CASCADE

R. A. Gomes - J. Kurz - R. Niehuis

Institute of Jet Propulsion
Universität der Bundeswehr München
85577 Neubiberg, Germany
reinaldo.gomes@unibw.de

ABSTRACT

Flow measurement using a linear compressor or turbine cascade is a well-established technique to characterize the flow in turbomachines with a certain degree of abstraction. A common way to obtain a general characterization of the flow is to measure the flow downstream of the cascade with a five-hole probe, obtaining e.g. total pressure losses and flow turning.

Pneumatic five-hole probes are used to capture steady or time-averaged flow quantities, if not otherwise specified. Using standard probes with considerable distance between probe head and pressure transducer, a dynamic calibration is possible, which allows to obtain a transfer function between measured pressure difference and actual pressure at the probe head. The transfer function is dependent on different effects such as overall pressure level and tube length between probe head and pressure transducer. Hence, for every different measurement set-up a dynamic calibration is necessary.

In this paper methods proposed by other authors are combined and extended to allow for fast or transient five-hole probe measurements, obtaining the transfer function directly from the measurement itself. The effectiveness of this method is presented for flow measurements downstream of a compressor cascade with attached and stalled flow (by varying the Reynolds number) as well as with steady and periodically unsteady inflow. The new method allows to reduce the measurement time by up to 90 percent without compromising measurement accuracy. In fact, due to higher spacial resolution, the flow downstream of the cascade can better be resolved with the new method.

KEYWORDS

Five-Hole Probe, Pneumatic Measurements, Linear Cascade

NOMENCLATURE

a, b	transfer function coefficients	q	stagnation pressure
c	chord length	Re	Reynolds number
C_s	Sutherland constant $= 1.458 \cdot 10^{-6} \text{ kg/(m}\cdot\text{s)}$	S	Sutherland constant = 110.4 K
d	diameter	T	temperature
l	tube length	t	pitch
Ma	Mach number	u	pitchwise coordinate, actual pressure
p	pressure	V	volume
		y	measured pressure

β	flow angle	δ	difference
γ	isentropic coefficient	μ	dynamic viscosity
Δ	uncertainty	ρ	density

INTRODUCTION

Pneumatic probes have been widely used in fluid mechanics research and are still a valuable measurement device for obtaining localized flow quantities such as total pressure, Mach number or flow angle. Its working principle relies on the relationship between flow velocity or Mach number and local static pressure changes. In turbomachinery research, pneumatic probes with two, three, five or even more holes are used to measure the flow properties in annular as well as linear cascades or even rotating rigs. The pressure at each of the holes is measured and the relation between the individual pressures allows to obtain the flow properties according to the values from a prior calibration.

For a standard pneumatic multi-hole probe the pressure is not measured directly at the holes. The hole is connected via small diameter tubes and hoses to the actual pressure transducer. At steady conditions the pressure inside the cavity of the pressure transducer is the same as at the hole. For a pressure change at the hole it takes a certain time to equalize the pressure difference between hole and pressure sensor. For accurate measurements one has to take this time lag into account when traversing a probe in a non-homogeneous flow. Depending on the kind of flow and the measurement set-up this time lag can be responsible for most of the time needed to measure a flow field. In order to reduce measurement time and hence the costs, it is important to find solutions which allow to minimize the settling time of the pressure changes. One way to shorten the measurement time is to use highly time-resolved pneumatic probes, where the pressure sensors are placed more or less directly at the probe tip. As drawbacks these probes are usually more expensive than standard probes, have larger dimensions, either at the probe tip or shortly downstream, to incorporate the sensors, can reduce the operating range due to build-in pressure sensors and are more difficult to handle.

If one wants to use a standard probe one can optimize the measurement set-up, as carried out e.g. in Grimshaw and Taylor (2016). Nevertheless such an optimization will face restrictions such as the size of the probe already in use and the minimum tube length from the probe to the sensor. Another or an additional way to reduce measurement time is to by-pass the pressure settling time by applying a transfer function to the pressure record as in Paniagua and Dénos (2002). For their method they traverse the probe continuously through the flow field and measure the pressure throughout the traverse. The pressure at the sensor is not allowed to settle down and is therefore not equal to the pressure at the probe tip. Since they made a prior calibration acquiring the response of the measurement set-up to a step change in pressure at the probe tip, they are able to reconstruct the actual pressure at the tip using a transfer function on the pressure history of the sensor. This method allows to reduce the measurement time considerably, but requires a calibration of the system to obtain the transfer function. Such a calibration has to be done not only for different measurement set-ups individually but also for different flow conditions. The absolute pressure level at which the system is working has a huge influence on the response of the system and measurements at different pressure levels require therefore individual calibrations. Such additional efforts may outweigh the advantages of a continuous measurement and hence are not suitable for measurements under strongly varying pressure levels.

At the High-Speed Cascade Wind Tunnel of the Institute of Jet Propulsion of the Armed

Forces University Munich, flow measurements with pneumatic probes using linear turbine and compressor cascades are often carried out for different operating points with a large variation of pressure level. A dynamic calibration for every measurement would represent an effort as high or even higher than a standard measurement of a traverse at mid-span waiting for the pressure settling time for each measurement point. In order to improve the overall time needed for the measurement, a transfer function based on the method of Paniagua and Dénos (2002) is applied to the measurement using the values of the measurement itself to obtain the transfer function.

SETTLING TIME AND TRANSFER FUNCTION METHOD

The determination of the settling time for pressure measurement systems with time lag between pressure changes at the measurement location and the measurement device has been case of study quite early in the history of wind tunnel testing. Sinclair and Robins (1952) develop an equation for the determination of settling time for laminar, incompressible flow measured by a manometer. The measured pressure at the measurement device — in the case of this reference a manometer but it can also be a pressure gauge — is a function of time $p = f(t)$. At $t = 0$ the system is in equilibrium at $p = p_0$. After a step change at the orifice of the measurement system (e.g. a probe tip) from p_0 to p_1 the measured value will change. The settling time can be defined as time needed for the measured pressure to level 99.9% of the initial pressure difference $p_1 - p_0$, i.e.

$$p_s = 0.999 \cdot p_1 + 0.001 \cdot p_0. \quad (1)$$

In Sinclair and Robins (1952) the settling time t_p is given as

$$t_p = \frac{128\mu l_e}{\pi d^4} \left[\frac{V}{p_1} \ln \frac{(p_0 - p_1)(p_s + p_1)}{(p_s - p_1)(p_0 + p_1)} + \frac{3V_d}{p_0 - p_1} \ln \frac{p_0 + p_1}{p_s + p_1} + \frac{V_d}{p_0 - p_1} \ln \frac{p_0 - p_1}{p_s - p_1} \right], \quad (2)$$

with the natural logarithm \ln , the total volume of the system V and the displacement volume due to fluid level change in the manometer V_d . The equivalent length l_e is determined for a combination of different tube diameters d_i by

$$l_e = l_1 + l_2 \frac{d^4}{d_2^4} + l_3 \frac{d^4}{d_3^4} + \dots + l_n \frac{d^4}{d_n^4}. \quad (3)$$

Larcombe and Peto (1966) derive the settling time for slip flow as

$$t_p = \frac{128\mu (V + kv) l}{\pi d^4 (p_1 + K)} \left[\ln \frac{p_1 + p_s}{p_1 - p_s} - \ln \frac{p_1 + p_0}{p_1 - p_0} + \ln \frac{1 + \frac{2K}{p_1 + p_s}}{1 + \frac{2K}{p_1 + p_0}} \right], \quad (4)$$

with

$$K = 8 \left(\frac{\pi}{2} \right)^{0.5} \left(\frac{2}{f} - 1 \right) \frac{\mu}{d \left(\frac{\rho}{p} \right)^{0.5}} \quad (5)$$

being f the fraction of gas molecules that is diffusely reflected suggested to be $f = 0.8$ for air at 20° C and kv equivalent to V_d in eq. (2). The equivalent length for combination of various diameters is given as

$$l_e = l + \sum_{i=1}^n \frac{l_i d^4 (p_1 + K)}{d_i^4 (p_1 + K_i)} \frac{\ln \frac{199p_1 + p_0 + 200K_i}{p_1 + p_0 + 2K_i}}{\ln \frac{199p_1 + p_0 + 200K}{p_1 + p_0 + 2K}}. \quad (6)$$

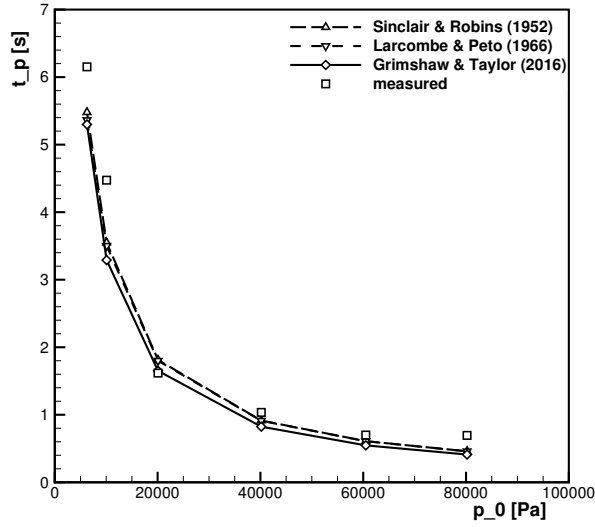


Figure 1: **Settling time as function of the initial pressure p_0**

In a recent publication Grimshaw and Taylor (2016) use an electric circuit analogy to derive the set of differential equations for determination of the pressure history. Though the results in their absolute values might differ from each other, they altogether show a strong dependency of the settling time from the absolute pressure level. Figure 1 shows the settling time dependency on the overall pressure level p_0 for a typical measurement configuration in a wind tunnel, applying the theories discussed so far. The strong increase of the settling time with decreasing pressure level seems evident. The configuration of the measurement set-up for a single pressure hole of the five-hole probe is explained in Table 1, while the applied pressures are given in Table 2. In overall the probe head has a diameter of 2.5 mm.

Some validation measurements were carried out with a simple set-up and a manual valve to produce a sudden pressure increase from p_0 to p_1 at the five-hole probe tip. A *Kulite* pressure sensor placed close to the probe tip is used as reference signal to capture the actual pressure increase. The fast reacting pressure sensor is of the type *XCQ-062* and has a natural frequency of 150 kHz with a differential pressure range of 350 hPa. In overall the measurements confirm the trend predicted by the cited authors as shown in Fig. 1. Viscous effects might be responsible for the slight increase in settling time in the experiments.

One may try to reduce the settling time as carried out e.g. in Sinclair and Robins (1952) or Grimshaw and Taylor (2016) by optimizing the tube diameters, but physical limitations and

	l	d
probe tip	5 mm	0.4 mm
probe stem	230 mm	0.55 mm
connecting tube	1000 mm	1.5 mm
transducer tube	100 mm	1 mm

Table 1: **Typical probe and connecting tubes dimensions for five-hole probe set-up**

p_0	$p_1 - p_0$
80,200 Pa	1,100 Pa
60,500 Pa	750 Pa
40,170 Pa	670 Pa
20,080 Pa	540 Pa
10,080 Pa	460 Pa
6,260 Pa	590 Pa

Table 2: **Pressure boundary conditions for evaluation of the settling time**

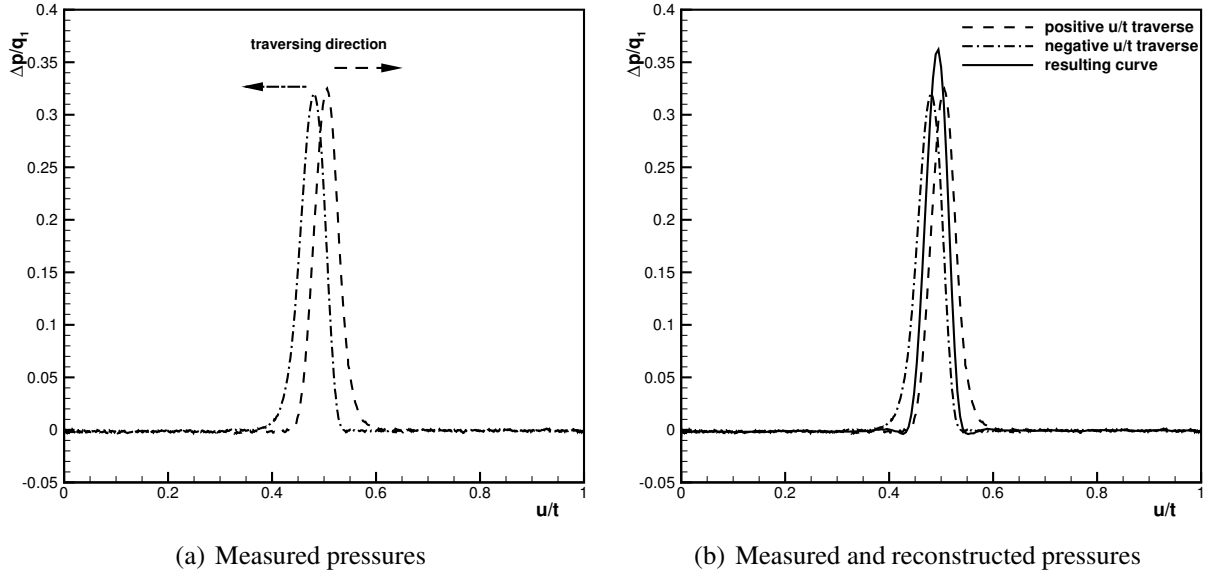


Figure 2: **Measured pressure difference between total inlet pressure and centre bore of the probe normalized by stagnation pressure and resulting normalized pressure difference as outcome of the transfer function**

constraints to the set-up will always lead to considerable time consumption of measurements with standard pneumatic probes, especially at low pressure levels.

Continuous Traverse Using Transfer Function

Paniagua and Dénos (2002) present a method using a transfer function to obtain the true pressure at the probe tip. Simplifying and neglecting any time delay between step change and pressure rise at the transducer one can reconstruct the true pressure from the time history of the true pressure and the measured pressure. For a measurement at a sampling time instance j the true pressure u is obtained by

$$u_j = -b_1 \cdot u_{j-1} - \dots - b_m \cdot u_{j-m} + a_0 \cdot y_j + a_1 \cdot y_{j-1} + \dots + a_m \cdot y_{j-m} \quad (7)$$

with the order of the function m and the measured pressure y . A probe might then be traversed continuously through an inhomogeneous flow field and the actual pressure at each of the holes reconstructed by the measured pressure. For such an operation one must know the coefficients $b_1 \dots b_m$ and $a_0 \dots a_m$, which can be obtained by prior calibration, as shown by the same authors. But if one is carrying out measurements at different pressure levels this would imply a calibration for each pressure level, which would outweigh any time savings by this method.

A more suitable way for measurements under varying pressure conditions is to obtain the coefficients from the measurement itself, bypassing any calibration. Therefore a method proposed by Bartsch et al. (2015) for optimization of the measurement point distribution for standard measurements is used here to determine the coefficients of the transfer function. In the publication from Bartsch et al. (2015) they perform two traverses in opposite direction downstream of an aerofoil in order to determine the wake position and to enhance the measurement point distribution for a standard traverse.

Such a dual traverse can also be used to obtain directly the actual pressure at each measurement location. In Figure 2(a) typical results for a dual traverse are plotted. The dashed

line shows the measured pressure difference between total inlet pressure and the pressure at the centre hole of the probe normalized by a random stagnation pressure for a continuous traverse toward higher u/t values. The dashed-dotted line shows similar readings for a traverse in the same flowfield but moving in opposite direction. It is evident that the time delay between actual pressure change and measured pressure leads to a phase lag of the measured pressure, seen in the different position of the peak values. Additionally, the measured pressure difference is expected to be lower than the actual maximum. The coefficients for the transfer function in Eq. (7) can be evaluated iteratively and the function applied to both traverses must give the same result, or more precisely

$$\mathbf{u}_f - \mathbf{u}_s = \Psi_f \cdot \boldsymbol{\varphi} - \Psi_s \cdot \boldsymbol{\varphi} = \boldsymbol{\xi} \quad (8)$$

with the vectors of the measured pressures $\mathbf{u} = [u_m, \dots, u_n]^T$ for n measurement points and with the subscripts f and s for the first respectively second traverse. The vector $\boldsymbol{\varphi} = [-b_1, \dots, -b_m, a_0, \dots, a_m]^T$ holds the coefficients of the transfer function while the matrix Ψ is defined as

$$\Psi = \begin{bmatrix} u_{m-1} & \cdots & u_1 & y_m & \cdots & y_1 \\ \vdots & & & & & \vdots \\ u_{n-1} & \cdots & u_{n-m} & y_n & \cdots & y_{n-m} \end{bmatrix}. \quad (9)$$

The coefficients of the vector $\boldsymbol{\varphi}$ in Eq. 8 are iteratively searched to minimize the root mean square of the error vector $\boldsymbol{\xi}$ using the *MATLAB* function *fminsearch*. The order of the function m can be individually set for each experiment, but in our measurements an order higher than $m = 3$ did not change the results significantly.

Since the number of coefficients for $\boldsymbol{\varphi}$ is in general higher than two, additional constraints are put into the algorithm for the iterative search: the resulting actual pressure history as function of u/t has to cross both measured pressure difference peaks. This is true, since the traversing velocity is moderate which results in pressure fluctuations far below unity. According to the works of Bergh and Tjeldeman (1965) or Carolus (1986) at such low frequencies and since the system is overdamped, no noticeable phase lag is perceived for the pressure reverse at the tip of the probe. The resulting pressure line for the curves shown in Figure 2(a) is plotted in Figure 2(b) together with the measured curves.

Such an iterative search can be done for all the holes or measured pressure differences of the five-hole probe and the actual flow values can be computed.

Error Estimation

An error estimation is more difficult to conduct using the transfer function since every computed pressure difference relies on the history of the measured and reconstructed pressure values $u_j = f(u_{j-1}, \dots, u_{j-m}, y_j, \dots, y_{j-m})$. This means that every error in previous samples propagates to the following pressures. Using the linear error propagation technique, which is the more conservative approach, without any further analysis would very soon increase the uncertainty towards infinity, since

$$\Delta u_j = |-b_1| \cdot \Delta u_{j-1} + \dots + |-b_m| \cdot \Delta u_{j-m} + |a_0| \cdot \Delta y_j + \dots + |a_m| \cdot \Delta y_{j-m}, \quad (10)$$

with Δy as the uncertainty of the pressure gauge, i.e. $\Delta y_j = \Delta y_{j-1} = \dots = \Delta y$. But one can overcome this problem if one separates the systematic from the random error with

$$\Delta y_j = \overline{\Delta y} + \Delta y'_j, \quad \text{with} \quad \sum_{j=1}^{\infty} \Delta y'_j = 0. \quad (11)$$

The systematic error is constant for all samples, therefore Eq. (10) can be rewritten as

$$\begin{aligned}\Delta u_j = & | -b_1 | \cdot \Delta u_{j-1} + \dots + | -b_m | \cdot \Delta u_{j-m} + \\ & | a_0 + \dots + a_m | \cdot \overline{\Delta y} + | a_0 | \cdot \Delta y'_j + \dots + | a_m | \cdot \Delta y'_{j-m}.\end{aligned}\quad (12)$$

The effect of such a method can be seen exemplary for a case of the order $m = 1$ for simplification. The first transformation is at the second sample

$$u_2 = -b_1 \cdot u_1 + a_0 \cdot y_2 + a_1 \cdot y_1 \quad (13)$$

$$\begin{aligned}\Delta u_2 &= | a_1 - b_1 | \cdot \Delta y_1 + | a_0 | \cdot \Delta y_2 \\ &= | a_0 + a_1 - b_1 | \cdot \overline{\Delta y} + | a_1 - b_1 | \cdot \Delta y'_1 + | a_0 | \cdot \Delta y'_2,\end{aligned}\quad (14)$$

since at the first sample the probe is not in motion and the measured pressure can be seen as the actual pressure at the probe tip $u_1 = y_1$. For the third reading the result from Eq. (14) is set into the error estimation of Eq. (12)

$$\begin{aligned}\Delta u_3 &= | -b_1 | \cdot \Delta u_2 + | a_0 | \Delta y_3 + | a_1 | \cdot \Delta y_2 \\ &= | (a_0 + a_1) \cdot (1 + b_1) - b_1^2 | \cdot \overline{\Delta y} + \\ & \quad | b_1(a_1 - b_1) | \cdot \Delta y'_1 + (| b_1 a_0 | + | a_1 |) \cdot \Delta y'_2 + | a_0 | \cdot \Delta y'_3.\end{aligned}\quad (15)$$

Applying the same method into the fourth reading gives

$$\begin{aligned}\Delta u_4 = & | (a_0 + a_1) \cdot (1 + b_1 + b_1^2) - b_1^3 | \cdot \overline{\Delta y} + \\ & + | b_1^2(a_1 - b_1) | \cdot \Delta y'_1 + (| b_1^2 a_0 | + | b_1 a_1 |) \cdot \Delta y'_2 + \\ & + (| b_1 a_0 | + | a_1 |) \cdot \Delta y'_3 + | a_0 | \cdot \Delta y'_4.\end{aligned}\quad (16)$$

Continuing the row one can easily find the relation

$$\begin{aligned}\Delta u_j = & \overline{\Delta y} \left| \sum_{n=0}^{j-2} (a_0 + a_1) b_1^n - b_1^{j-1} \right| + \\ & \sum_{n=2}^{j-1} \Delta y'_n (| a_0 \cdot b_1^{j-n} | + | a_1 \cdot b_1^{j-n-1} |) + \Delta y'_0 | a_1 \cdot b_1^{j-2} - b_1^{j-1} |.\end{aligned}\quad (17)$$

The first summand of Eq. (17) can be brought to a geometric series for $b_1 \neq 1$ with

$$\overline{\Delta y} \left| \sum_{n=0}^{j-2} (a_0 + a_1) b_1^n - b_1^{j-1} \right| = \overline{\Delta y} \left| (a_0 + a_1) \frac{b_1^{j-1} - 1}{b_1 - 1} - b_1^{j-1} \right|.\quad (18)$$

Equation (18) does not converge for $|b_1| > 1$. It is therefore mandatory to find coefficients b_n where the sum of the absolute values is smaller than unity in order to maintain mathematically correctly the uncertainty at low levels. Otherwise the uncertainty grows exponentially with the number of data points.

The fluctuating random error in Eq. (17) can be in general neglected for the average values, since the sum of the errors is equal to zero and the fluctuations are essentially due to the noise.

Doing so the measurement accuracy for standard and new measurement techniques is 0.01 for the Mach number measured by the five-hole probe, 0.1° in β and approximately 10% of ζ .

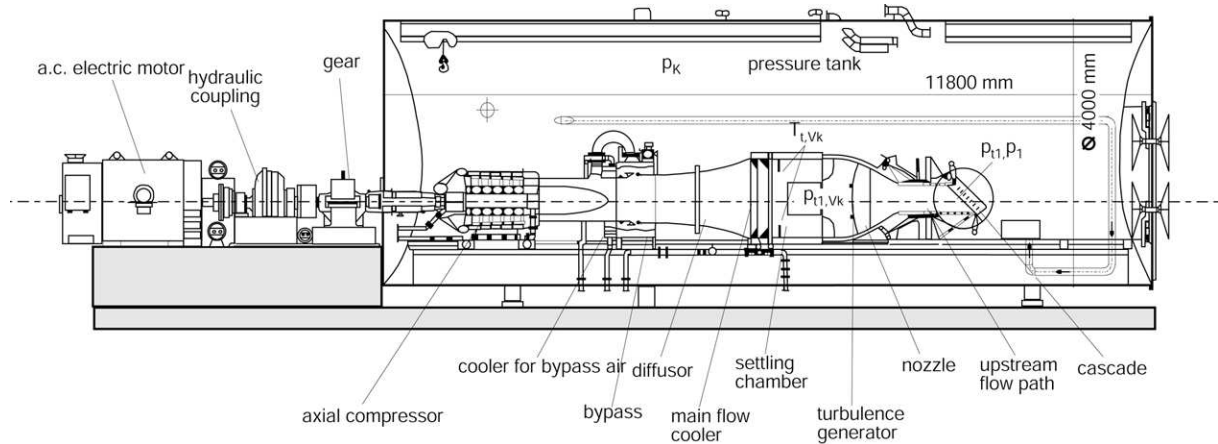


Figure 3: Drawing of the High-Speed Cascade Wind Tunnel

TEST SET-UP

The experiments with a linear cascade were performed at the High-Speed Cascade Wind Tunnel of the Institute of Jet Propulsion at the Armed Forces University Munich. A drawing of the tunnel is given in Figure 3. The main components of the facility are a six-stage axial compressor, a settling chamber with laminar coolers and the nozzle. These parts are enclosed inside a pressure chamber where the static pressure can be changed between 3,000 Pa and 120,000 Pa. Controlling the compressor speed and the cooling of the air, the flow Mach and Reynolds numbers can be varied independently from each other. The Mach number range at the nozzle exit lies within $0.1 \leq Ma \leq 1$ and the range of the Reynolds number based on nozzle exit conditions divided by the geometric scale is approximately $2 \cdot 10^5 \text{ m}^{-1} \leq Re/l \leq 16 \cdot 10^6 \text{ m}^{-1}$.

The compressor is driven by a 1.3 MW electric motor and the speed is controlled by a hydraulic coupling. These components are placed outside of the pressure chamber. Further details on the facility can be found in Sturm and Fottner (1985).

Periodic Wake Generation

The interaction of the flow around the profile with periodically impinging wakes from an upstream moving aerofoil can be simulated with cylindrical bars. The wake generator is placed at the nozzle exit and the cascade inside the wake generator. Cylindrical bars are moved linearly upstream of the cascade and parallel to it. After passing the circumferential end of the cascade the bars do a 180° turn and move backwards downstream of the cascade at sufficient distance not to interact with the outflow from the cascade. After a second turn the cycle reinitializes. The wake generator was run at 40 m/s with a bar distance of 80 mm resulting in a frequency of 500 Hz of the wake disturbance. Details about the design can be found in Acton and Fottner (1996).

Data Acquisition and Post Processing

The operating point of the cascade is controlled by the static pressure at the inlet to the cascade and the local stagnation pressure. The static pressure p_1 is measured with pressure taps at the sidewall of the nozzle, while the stagnation pressure q_1 is measured with a pitot probe in the nozzle. With these two pressures the Mach number is computed assuming adiabatic isentropic expansion.

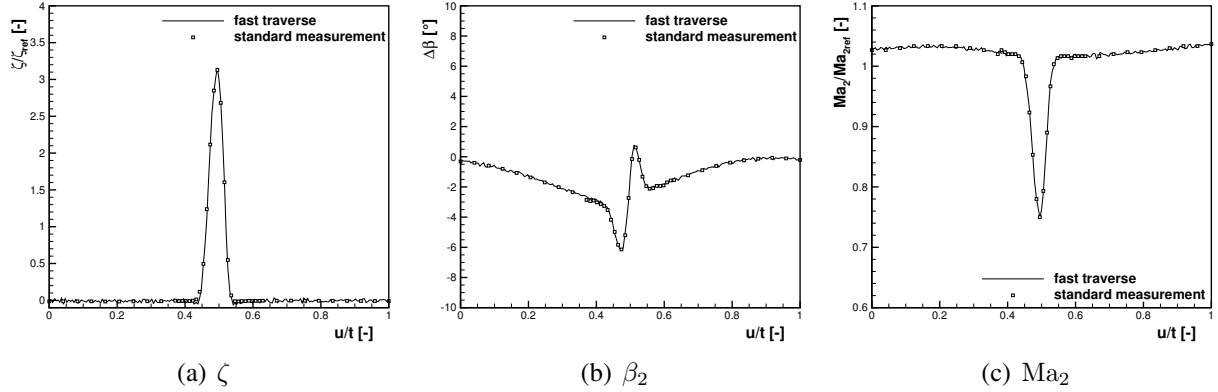


Figure 4: Flow properties measured downstream of the cascade with standard and fast traverse technique for medium Reynolds number and steady inflow

The Reynolds number is the second similarity parameter which is controlled using the definition

$$Re = \sqrt{\frac{\gamma}{R} \frac{c}{C_s}} \frac{Ma \cdot p_1 \cdot \left(\frac{T_{t1}}{1 + \left(\frac{\gamma-1}{2}\right) \cdot Ma^2} + S \right)}{\left(\frac{T_{t1}}{1 + \left(\frac{\gamma-1}{2}\right) \cdot Ma^2} \right)^2}. \quad (19)$$

The total temperature of the flow T_{t1} is measured with four PT100 resistance thermometers inside the settling chamber.

The downstream flow is measured with a five-hole pneumatic probe. The pressures at the five holes give the coefficients which allows to obtain the local Mach number Ma_2 , the local total pressure p_{t2} and the flow angle in circumferential direction β_2 . The total pressure is used to compute the profile losses defined by

$$\zeta = \frac{p_{t1} - p_{t2}}{q_1}. \quad (20)$$

Due to confidentiality reasons the values are normalized by a random reference value or, in case of the flow angle, given as difference from a reference value.

The integral values over one complete pitch are computed as mixed out values using the method of Amecke (1967) where the conservation of mass, moment and energy is fulfilled.

EXPERIMENTAL RESULTS

The new method was applied on measurements downstream of a linear compressor cascade with moderate turning and a Mach number at the outlet of approximately 0.3. A broad range of Reynolds numbers were investigated but for brevity only results from two Reynolds numbers are shown here: a medium Reynolds number of 150,000 at which low profile loss is generated and a low Reynolds number of 50,000 where stalled flow is present. The method is shown to work also with periodically unsteady inflow.

Results from a traverse at a medium Reynolds number and steady inflow conditions are given in Figure 4. The normalized profile losses, the flow angle difference, and the normalized Mach number are given as function of the relative pitchwise position. The results from a standard traverse are given as symbols and the ones from a fast traverse are drawn as lines. It is

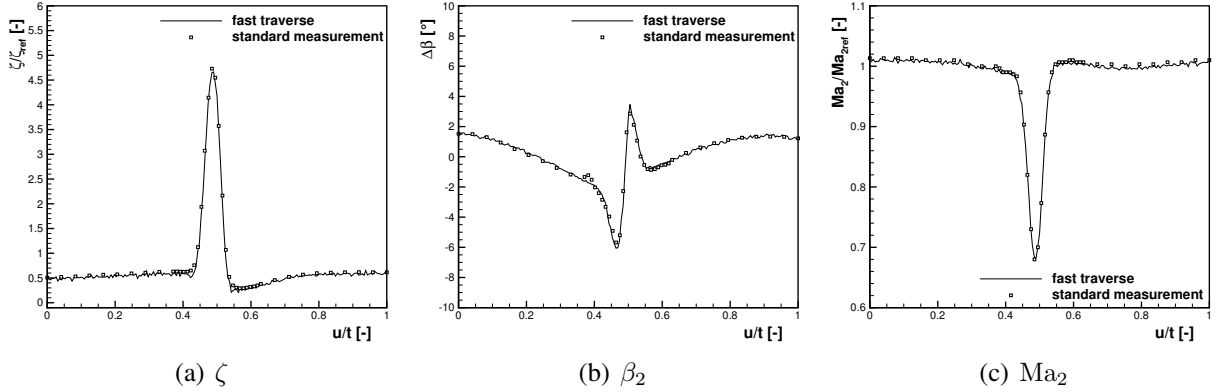


Figure 5: Flow properties measured downstream of the cascade with standard and fast traverse technique for medium Reynolds number and periodically unsteady inflow

flow property	steady inflow	unsteady inflow
$\delta\zeta/\zeta$	0.00025	0.00059
$\delta\beta$	0.03°	$< 10^{-2}$
δMa	$< 10^{-3}$	0.001

Table 3: Differences of integral values using standard and fast traverse technique

visible that at these conditions both measurements give very similar results along the pitch and all extreme values as well as gradients are matched.

The results of the transient measurements shown here are for a traversing velocity of 2 mm/s. The same operating point was measured with a traversing velocity of 1 mm/s. In the latter case the acquired pressures are closer to the actual values but after transformation with Eq. (7) the results are similar for all three cases.

The method was also applied to measurements with unsteady inflow. Figure 5 depicts the flow properties downstream of the cascade for the same Reynolds number but with unsteady inflow. Also here the differences are negligible. One should note that in Figure 5 the total pressure losses produced by the wake generator are included in the profile loss curve and that the scale of the ordinate was changed.

The difference in integral values between standard and fast measurement technique is given in Table 3. The differences are well below the measurement accuracy. The method described here seems therefore to be reliable.

More difficult to measure are operating points with very low Reynolds numbers due to the low absolute pressures. Nevertheless the method gives decent results when comparing to the standard technique in Figure 6. Only the flow angle is computed considerably different with an offset of 0.4° , but this could also be due to a slight change in the operating point at completely stalled flow.

The measurement time decrease is depicted in Figure 7 for low and medium Reynolds number cases. The total time needed is normalized by the time needed at the low Reynolds number with standard technique. One can see that the new technique can decrease the total time needed for one traverse by up to 90%. For a better estimate of the time saved: the typical overall measurement time for a standard traverse at low Reynolds number is approximately 45 minutes.

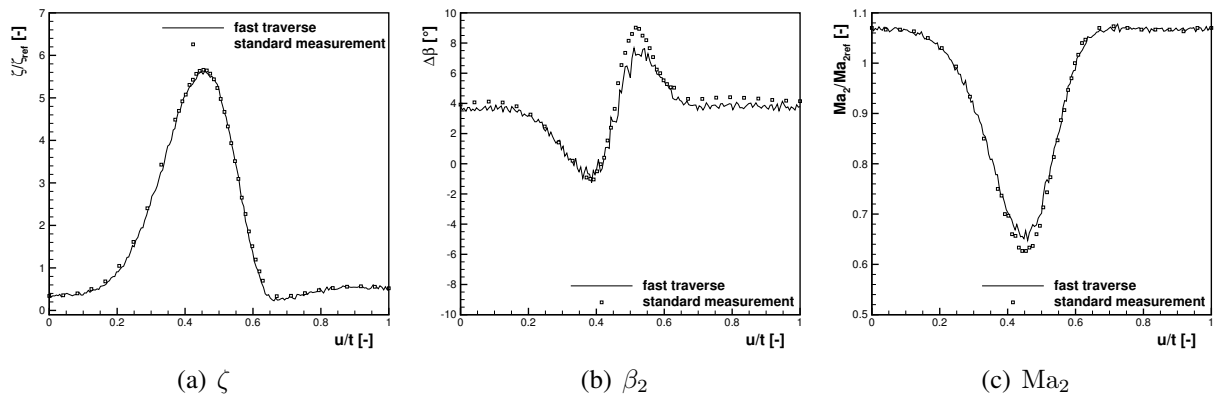


Figure 6: Flow properties measured downstream of the cascade with standard and fast traverse technique for low Reynolds number and periodically unsteady inflow

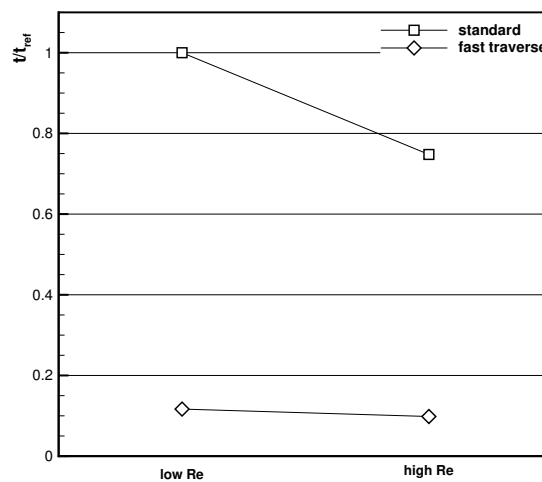


Figure 7: Total measurement time needed for a complete traverse

The same technique was also applied to measurements downstream of a transonic turbine cascade and the results are similarly encouraging.

CONCLUSIONS

This paper presents a new method to measure the flow downstream of a cascade with a standard five-hole probe. The new method is based on obtaining a transfer function from two traverses with the direction of probe movement in opposite direction.

The technique presented here has been tested on compressor and turbine cascades and allows to decrease the total measurement time by up to 90% without noticeable loss in accuracy. In fact due to a better spatial resolution of the flow, the accuracy can be increased for specific cases.

An extensive error analysis on measurements using a transfer function is performed. The analysis shows the way to obtain proper coefficients to reduce the measurement uncertainty. If no care is paid to this, the uncertainty will grow exponentially with increasing number of data points.

ACKNOWLEDGEMENTS

The authors wish to thank Mr. Wilfried Ehrlich and Mr. Franz Grabendorfer for running the test facility and the valuable input for the measurements.

REFERENCES

- P. Acton and L. Fottner. The Generation of Instationary Flow Conditions in the High-Speed Cascade Wind Tunnel of the German Armed Forces University Munich. In *13th Symposium on Measuring Techniques*, Zurich, Switzerland, 1996.
- J. Amecke. Auswertung von Nachlaufmessungen an ebenen Schaufelgittern. Technical Report 67 A 49, AVA Göttingen, 1967.
- C. Bartsch, M. Hölle, P. Jeschke, and T. Metzler. 1d adaptive measurement grid for improved pneumatic probe measurements. In *ASME-Paper GT2015-42352*, 2015.
- H. Bergh and H. Tijdeman. Theoretical and experimental results for the dynamic response of pressure measuring systems. NLR-TR F.238, National Aero- and Astronautical Research Institute, 1965.
- T. Carolus. Kunststoffleitungen zwischen druckmeßstelle und druckaufnehmer als fehlerquelle bei der messung instationärer drucksignale. *Forschung im Ingenieurwesen*, 52:191–197, 1986.
- S. Grimshaw and J. Taylor. Fast settling millimetre-scale five-hole probes. In *ASME Paper GT2016-56628*, 2016.
- M. Larcombe and J. Peto. The response times of typical transducer-tube configurations for the measurement of pressures in high-speed wind tunnels. C.P. 913, Aeronautical Research Council, 1966.
- G. Paniagua and R. Dénos. Digital compensation of pressure sensors in the time domain. *Experiments in Fluids*, 32:417–424, 2002.
- A. R. Sinclair and A. W. Robins. A method for the determination of the time lag in pressure measuring systems incorporating capillaries. Technical Note 2793, NACA, 1952.
- W. Sturm and L. Fottner. The High-Speed Cascade Wind-Tunnel of the German Armed Forces University Munich. In *8th Symposium on Measuring Techniques for Transonic and Supersonic Flows in Cascades and Turbomachines*, Genova, Italy, October 1985.